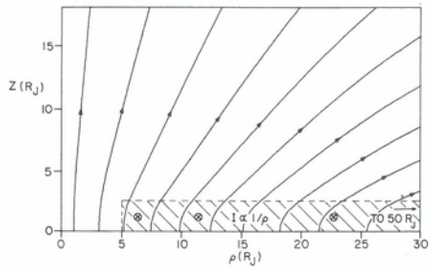

Fig. 1.22. Meridian plane plot of field lines associated with the magnetodisc current sheet model of Connerney, Acuña, and Ness [1981].

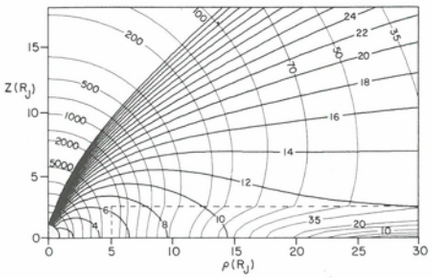

Fig. 1.23. Meridian plane projection of magnetosphere field lines (heavy) and isointensity contours (light) for Voyager 1 (and Pioneer 10) model of Connerney, Acuña, and Ness [1981]. Values on field lines indicate colatitude of field line; field magnitude contours are expressed in nanoteslas.

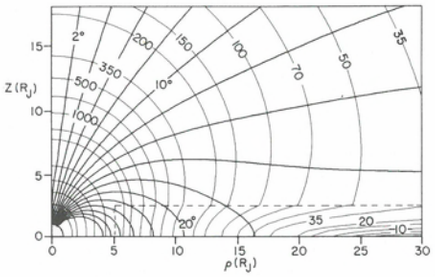

Fig. 1.24. Meridian plane projections of magnetosphere field lines (heavy) and isointensity contours (light) for Voyager 1 (and Pioneer 10) model of Connerney, Acuña, and Ness [1981]. Values on field lines indicate equatorial distance of field line crossing in absence of magnetodisc current sheet. Field magnitude contours are given in nanoteslas.

Discussion

All of the magnetic field models, with the exception of the Engle and Beard [1980] model, have assumed azimuthal symmetry. Goertz et al. [1976] fit the observed P 10 field magnitude outbound at ~0500 local time, whereas Barish and Smith [1975] fit the observed P 10 inbound field magnitudes at ~1000 local time. These models apply on either of the inbound or outbound passes only and are not used for both. Connerney, Acuña, and Ness [1981] also noted a departure from azimuthal symmetry evident in the V 1, V 2, and P 10 observations within 30 R_J. Because they used vector observations instead of field magnitudes, they were able to determine that the radial field component was primarily responsible for the inbound/outbound asymmetry, the inbound radial component being ~1/3 less than the outbound radial component. The observed vertical field component, however, did not show an inbound/outbound asymmetry. This, they suggested, could readily be explained by a thickening of the annular current sheet in the dayside magnetosphere, that is, a displacement to higher latitudes of ~1/3 of the azimuthal current. This possibility is supported by P 10 (inbound) observations of 1.79–2.15 MeV protons [Northrop, 1979], which indicate a thickening of the dayside plasma sheet. Additionally, Voyager observations [McNutt et al., 1981] of

plasma fluxes toward the magnetic equator at local midnight and away from the magnetic equator at local noon provide direct and independent evidence of such a dayside thickening.

The Euler potential models are most useful in providing an uncomplicated analytical description of field line morphology facilitating studies of particle motion or field line motion (e.g., Stern [1970]). They are less useful in providing insight into the large-scale current systems responsible for the magnetodisc magnetic field. Goertz et al. [1976] and Jones, Melville, and Blake [1980] have noted that the Euler potential models imply (by taking the curl of the modeled field) unphysical currents in certain regions of space, for example, infinite currents at the origin or large currents at great distances. The model of Barish and Smith [1975] is a good example of how these fictitious currents arise. Their model uses a dipolar field at high latitudes plus an additional term effective only at low latitudes to stretch out the field lines along the equator. The model results in azimuthal currents in the equator to pull the field lines radially outward, but also azimuthal currents at higher latitudes of the opposite sign. The currents are essentially required to cancel the magnetic field of the equatorial currents so that the total high latitude field is dipolar. In this example, the current system obtained is largely a result of the unreasonable requirement that the magnetic field of the equatorial current sheet be localized to lower latitudes. Such features make the estimates of local current density (in the magnetodisc) untrustworthy, unless it can be shown that the contributions to the observed magnetic field of all other currents is small. Clearly, it is necessary to exercise caution in the interpretation of the quantity $\overline{\nabla} \times \mathbf{B}$ computed from the Euler potential models. For the same reason, caution is also advised in extrapolation of the field away from the equatorial region using the Euler potential models.

Consequences of a magnetodisc field morphology

Each of the magnetic field models describes a magnetodisc field geometry in which field lines are radially stretched along the plane of symmetry of the azimuthal current disc (the magnetic equator in the models of Goertz et al. [1976] and Connerney, Acuña, and Ness [1981]). Phenomena that are sensitive to the field line morphology, such as the absorption of charged particles by satellites and the magnetopause surface geometry, are essentially consequences of the gross magnetodisc magnetic field geometry. Any of the models exhibiting the magnetodisc geometry would suffice to illustrate qualitatively such phenomena; for convenience we choose to utilize the model of Connerney, Acuña, and Ness [1981] in our discussion of charged particle absorption and auroral effects.

The magnetic field of the Jovian azimuthal current system is comparable in magnitude to the field of internal origin at a radial distance of ~15 R_J. At greater distances the resultant vertical field is much smaller than the radial component of the sheet field; thus the field is largely radial above and below the sheet. At 30 R_J, the field magnitude is twice that expected of a 4.2 G-R_J^3 dipole, and it is due almost entirely to the radial component of the sheet field. Thus, in magnitude and configuration the distant field is dominated by the annular current sheet.

We envision a Jovian magnetopause surface that is everywhere extended along the magnetic equator, that is, flattened in the direction of the Jovian dipole axis. This is entirely consistent with the static model calculations of Engle and Beard [1980] who assumed a rather different equatorial current sheet in their determination of the magnetopause surface. Indeed, the observations of Lepping et al. [1981] of 10-hr periodicities in the antisolar magnetosheath are understood in terms of the dynamics of a

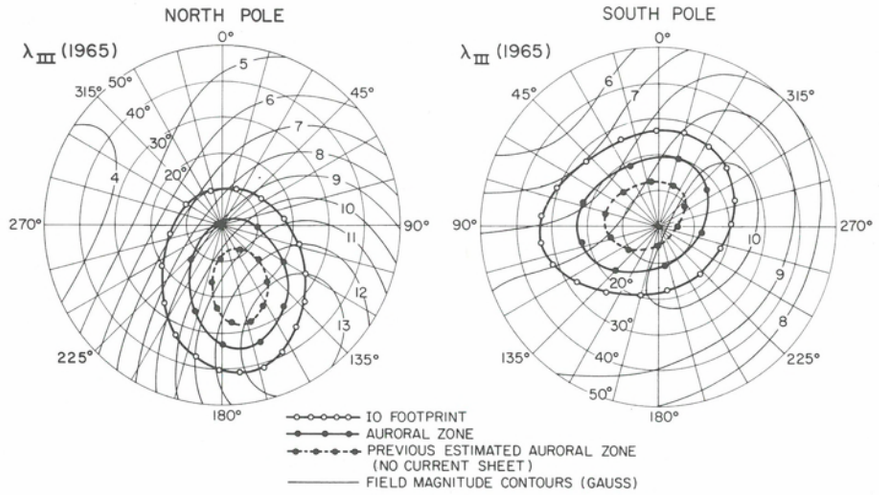

Fig. 1.25. Comparison of Io flux tube footprint for O_4 model with location of auroral zones computed with and without the magnetodisc current sheet. (The Io flux tube footprint is enlarged by a small amount [$< 2°$] when the magnetodisc currents are included. Only field lines at higher latitudes are significantly affected.)

flattened magnetopause surface. The five and ten hour periodicities in field magnitude, direction, and bow shock/magnetopause observations at greater distances all can be regarded as a consequence of the 10-hr "rocking" of the azimuthal current system due to the misalignment of the Jovian rotational and magnetic axes (see Sec. 1.4).

Another interesting consequence of the annular current sheet concerns the mapping of field lines from the (magnetic) equatorial plane to the planet's surface. Field lines at lower latitudes are unaffected by the presence of sheet currents, to $L \sim 6$. The radial stretching of higher latitude field lines results in a very narrow range of latitudes on the Jovian surface that map onto, or link to, the magnetodisc. In Figure 1.25 we show the intersection of the last closed field lines corresponding to the model magnetosphere illustrated in Figure 1.24 with the oblate surface of Jupiter. We have assumed the O_4 internal field model and simply traced field lines from just above the sheet at $\sim 30\ R_J$ down to the Jovian cloud tops. All of the field lines linking to the magnetodisc in this model originate between the Io footprint and the "auroral zone" footprint on the surface of Jupiter. Although we have tentatively identified the foot of the "last closed field lines" as the Jovian auroral zone, it is necessary to bear in mind that the asymmetries that have been neglected here, for example, the tail and magnetopause currents, are important in the determination of the auroral zone. In particular, we anticipate a dynamic situation, in which a variable Jovian auroral zone moves about within the indicated auroral zone in response to the 10-hr "rocking" of the azimuthal current sheet. A further variability in the size of the auroral oval may result if the azimuthal currents undergo a significant time variation, or as the tail and magnetopause currents change in response to solar wind variations.

The current sheet has important implications for charged particle motion in the Jovian magnetosphere, particularly in the absorption of trapped radiation by satellites. The stretching of the magnetic field lines in the magnetic equatorial plane leads to a significant distortion of the charged particle drift shells away from the simple quasidipolar geometry derived from the internal field model calculations for radial distances greater than $\sim 6\ R_J$. A complete description of charged particle motion requires

knowledge of the magnetic field line geometry and the field gradient and curvature drifts over the particle's bounce path and longitudinal drift motion. Such a drift-shell tracing computation including the effects of the current sheet given in this chapter is impractical due to the numerical labor and computer time required. For the purposes of this discussion, it will suffice to address the "radial distance to the equatorial point" associated with each magnetic field line. This identifies the equatorial crossing point of a field line, determined by numerically tracing the field line to the equator. Although useful for discussing some aspects of satellite absorption of charged particles (e.g., possible absorption event times), such a field-geometric approach does not benefit the study of energy, species and time dependencies inherent in satellite absorption signatures. In studying the geometry of trapped particle drift shells, it is customary to identify the field lines by their "L-value." Such terminology is only valid for strictly dipolar or quasidipolar fields and is not applicable to the highly distorted equatorial fields associated with the current sheet. The reader is referred to Roederer [1970] and Stern [1976] for extended discussions on the subject.

Qualitatively, the stretching of field lines in the magnetic equatorial plane implies that the charged particle absorption features created by the sweeping effect of the Jovian satellites can occur at radial distances far removed from those predicted by the internal field models. The timing and duration of the absorption event(s) depends on the positions of the satellite and observing spacecraft relative to the magnetic equator. The inclusion of the current sheet field must result in significantly broader particle absorption regions (in radial extent) where the radial magnetic field component is large. Figure 1.26 clearly illustrates these effects for the case of the V 2 encounter trajectory. For comparison, we have shown the radial distance to the equatorial point of magnetic field lines encountered by the spacecraft for both the O_4 model and a model including the current sheet [Connerney, Acuña, and Ness, 1981] as a function of time. Also shown is the range of radial distances (to the equatorial point) of field lines encountered by Ganymede in one Jovian day for both models of the magnetic field. Several interesting results can be derived from the figure. The inclusion of the current sheet field significantly enhances the "wobbling effect" of the magnetic field past the spacecraft. This increases the radial range of magnetic field lines that are morphologically connected to the spacecraft over that predicted by the internal field model alone. In the case of the Ganymede absorption, this effect is dramatic, owing to Ganymede's motion relative to the current sheet (Ganymede traverses the entire sheet width twice each rotation) and the near radial geometry of the field at $\sim 15\ R_J$. The time interval during which V 2 is located within the Ganymede sweeping region is extended from a few tens of minutes predicted by the internal field model to over *5 hours* for the model including the current sheet. Note that V 2 entered (briefly) the expanded absorption region at $\sim$0400 SCET, and again approximately 5 hr later; in the absence of a current sheet the absorption region is encountered only once, briefly, near 0900 SCET. In this case, the sweeping region is defined as the range of radial distances to the equatorial point of magnetic field lines which are connected to Ganymede around its orbit. This effect is, we expect, largely responsible for the location and extent of the plasma voids observed near Ganymede by V 2 on the inbound leg [Burlaga, Belcher, and Ness, 1980] from 0400–1200 SCET.

Although the model used here does not include the effects of the magnetopause or tail currents, it is clear from the figure that at times the radial distance to the equatorial point of the field line connected to the spacecraft can become comparable to the magnetopause radial distance or the "hinge" point in the Jovian tail. This exercise is similar to the identification of "open field lines" by Goertz et al. [1976] along the P 10 trajectory outbound.

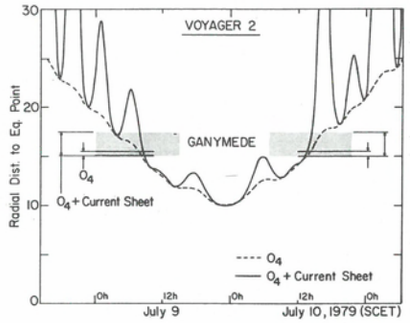

Fig. 1.26. The radial distance to the equatorial point of magnetic field lines encountered by Voyager 2 as computed from the O_4 model and the model including the current sheet field.

The results given here are necessarily approximate owing to the variability to the ring current and the external effects associated with the magnetopause and solar wind compression of the magnetosphere. In addition, the assumption of an axisymmetric ring current is only partially satisfied in the Jovian magnetosphere because the models given here point to a significant day–night asymmetry. This, of course, leads to significant drift-shell splitting, drift-loss cones and quasistable trapping regions. The radially stretched magnetic field geometry in the vicinity of the equatorial plane leads to an enhancement of the relative maxima observed in charged particle fluxes when traversing the magnetic equator. These effects, as observed by P 10 [Van Allen et al., 1974a], led to the initial concept of the magnetodisc (see also Sec. 1.4).

Nonmeridional field

In addition to, and quite distinct from, the radial extension of field lines in meridional planes due to azimuthal currents, Smith et al. [1975] observed a (westward) warping of the magnetic field lines out of meridional planes, most evident on the P 10 outbound trajectory near the dawn meridian. The P 10 inbound observations, as well as the P 11 (inbound and outbound) observations in the late morning sector of Jupiter's magnetosphere, demonstrated considerably less warping and less regular behavior. The P 10 outbound observations taken alone seem to suggest a spiral magnetic field configuration [Smith et al., 1975] reminescent of the Parker spiral of the solar wind. The assumed spiral field configuration was interpreted as evidence for the centrifugally driven planetary wind of Hill, Dessler, and Michel [1974] beyond the critical Alfvén radius of 30 R_J (for a review of outflow models see Kennel and Coroniti [1977a]). More recently, Hill [1980] has revised his estimate of the critical Alfvén radius to 20 R_J, based on V 1 plasma observations [Bridge et al., 1979a]. Empirical models of the azimuthal magnetic field, appropriate to the P 10 outbound pass only, are given by Goertz et al. [1976] and Jones, Melville, and Blake [1980]. A spiral configuration of the magnetic field was inferred also from the P 10 energetic particle flux modulation observed along the outbound trajectory [Northrop, Goertz, and Thomsen, 1974].

Assuming azimuthal symmetry, Parish, Goertz, and Thomsen [1980] found a radial current of $\sim 6 \times 10^7$ A in Jupiter's equatorial plane necessary to fit the P 10 outbound azimuthal field component. Connerney [1981b] proposed a physically more intuitive model of a polar inflow, equatorial radial outflow current system, requiring $\sim 10^8$ A, but questioned the assumption of azimuthal symmetry essential to either determination.

Observations by V 1 and V 2 [Ness et al., 1979a,b,c] outbound at 0400 and 0240 local time, respectively (midtail-transit positions), demonstrated unambiguously the development of an extensive Jovian magnetic tail (see Sec. 1.4 for a complete discussion) and not a spiral magnetic field configuration. Thus the deviation of the magnetic field lines from meridional planes appears to be driven by the solar wind interaction rather than Jupiter's rotation. Magnetic field lines are swept back in the antisolar direction and approach the direction of the magnetopause near that boundary. The so-called spiral field configuration observed by P 10 outbound was largely an artifact of the sample of observations in the dawn meridian. None of the aforementioned models reflect the appropriate symmetry (about the noon–midnight meridian plane), and therefore none are applicable in general to the Jovian magnetosphere. The model of Engle and Beard [1981] possesses the appropriate meridional symmetry but lacks a dusk to dawn tail current required by the observations. In a recent reanalysis of all Pioneer passes Jones, Thomas, and Melville [1981] proposed a model current system consisting of an equatorial azimuthal disc current and an equatorial dusk to dawn current extending well into the dayside magnetosphere. A more complete discussion of the Jovian magnetotail is found in Section 1.4.

1.4. The outer magnetosphere

Dayside outer magnetosphere

In the outer magnetospheric regions the cylindrical symmetry prevalent in the inner regions disappears due to the effects of the solar wind interaction with the magnetosphere. We thus have to differentiate between a "sunward side" outer magnetosphere and a "magnetospheric tail" extending away from the planet in the antisolar direction. The description and discussion of the outer magnetosphere on the *sunward* side of Jupiter will be restricted to the magnetospheric region denoted as "outer zone" in Figure 1.27 (also see Fig. 1.37). This zone just inside the magnetopause (MP) was described by Smith et al. [1975] on the basis of Pioneer observations as a region of irregular magnetic field with, however, a persistent southward component indicative of a closed magnetosphere. According to Davis and Smith [1976], during the Pioneer encounters it was a region approximately 15 R_J thick, at least near the equator, with a field strength of ~ 5 nT. The average field magnitude observed by V 1 in that region was ~ 16 nT for a final MP crossing at 47 R_J, and at the time of the V 2 encounter the field strength there was ~ 7 nT on average for a final MP traversal distance of ~ 62 R_J. Smith, Fillius, and Wolfe [1978] have concluded that when the Jovian magnetosphere is at its greatest extent, most of the field just inside the MP is not derived from the planetary (dipole) field, but from currents within the magnetosphere, the major contributor probably being the equatorial current sheet. When the magnetosphere is compressed, as during the passage of a high speed stream in the solar wind, the relative contribution of the planetary dipole field to the field near the magnetopause becomes increasingly signficant, increasing, for example, from a contribution of $\sim 20\%$ at 100 R_J to $> 40\%$ at 50 R_J.

The Voyager spacecraft also observed the outer zone to be approximately 15 R_J thick and to consist of predominantly southward fields, as illustrated in Figure 1.27*b*, which shows V 2 inbound 1-hr average magnetic field vectors projected on the plane containing the planet–Sun line and the magnetic dipole axis. At ~ 45 R_J, the field is seen to become more nearly parallel to the equatorial plane and then to increase in steepness relative to that plane outside the equatorial current sheet as the planet was approached. The field geometry observed by V 1 and V 2 inbound in the outer Jovian magnetosphere is thus in qualitative agreement with the closed magnetosphere model discussed by Smith, Davis, and Jones [1976] and shown schematically in Figure 1.27*a*.

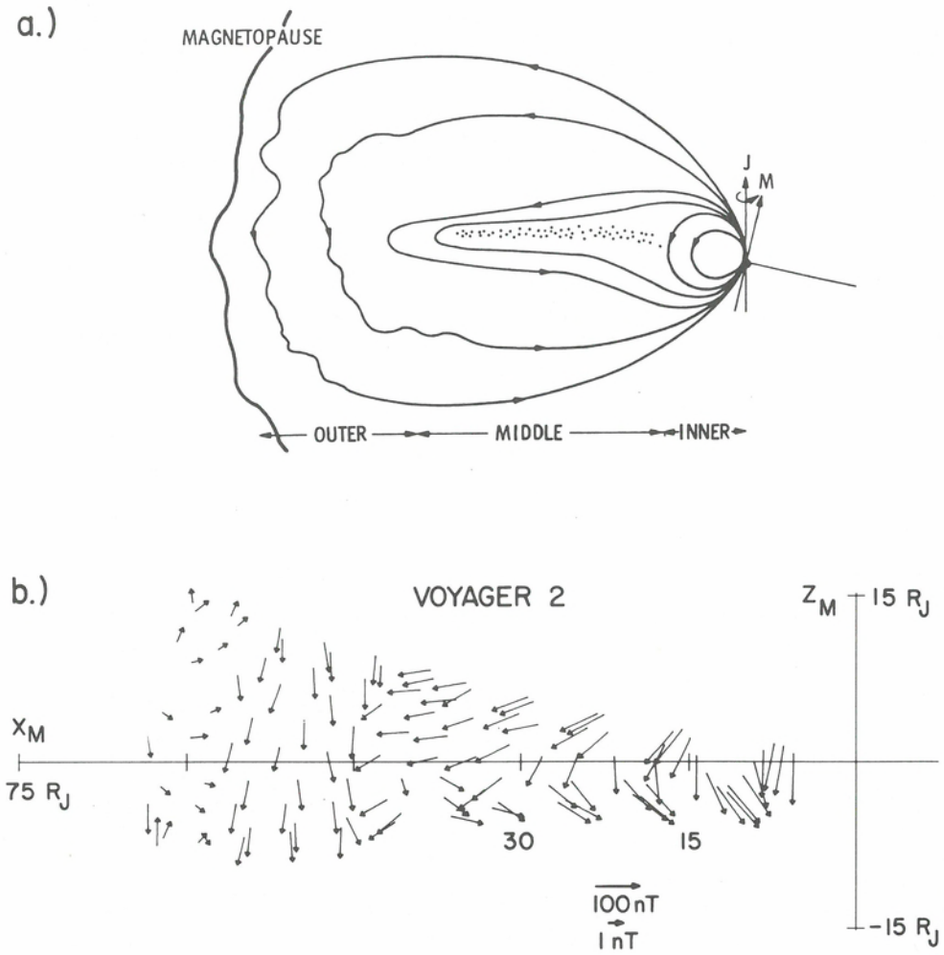

Fig. 1.27. (a) Closed Jovian magnetosphere model based on Pioneer observations [Smith, Davis, and Jones, 1976]. For Pioneer the inner region extended to ~20 R_J, the middle to ~60 R_J, and the outer to ~90 R_J. For Voyager the dimensions were ~15 R_J, ~45 R_J, and ~60R_J, respectively (Voyager 1's data were similar to Voyager 2's).
(b) Projection of hourly average vector magnetic field on the dipole coordinate x–z plane along the Voyager 2 trajectory inbound at Jupiter. In the dipole system, z_M is parallel to the magnetic dipole axis of Jupiter, positive northward, and the x_M and y_M axes lie in the magnetic equatorial plane such that the x_M–z_M plane contains the planet–Sun line, x_M positive toward the Sun.

In this view, the high latitude field lines are displaced outward by the presence of the equatorial current sheet and combine with current sheet and MP current fields to form the relatively "soft" zone of predominantly southward fields between the outer edge of the current sheet and the MP. It is the trapped plasma associated with the current sheet which ultimately must balance the pressure of the external thermalized sheath plasma. The "buffer" zone between the edge of the current sheet and the MP is very sensitive to variations in external pressure, functioning as a shock-absorber for fluctuations of small to moderate amplitude but allowing large-scale compression of the dayside magnetosphere in the presence of major perturbations, as illustrated by differences in the scale of the dayside magnetosphere observed by the Pioneer and the Voyager spacecraft.

Although we have defined here the thickness of the outer zone to be approximately 15 R_J as suggested by the Pioneer and Voyager magnetic field observations, this only applies to the inner part where relatively steady, southward pointing fields are seen. Although southward-directed on average, the fields nearest the MP are highly variable and disorganized on shorter timescales (the left-most, nonsouthward-directed hourly data in Figure 1.27*b* are a mix, however, of magnetosheath, magnetosphere and a small fraction of interplanetary data). This outer region in particular can vary significantly in radial extent, resulting in a sunward magnetopause distance at least as great as ~100R_J [Smith et al., 1975; Smith, Fillius, and Wolfe, 1978; Trainor et al., 1974; Van Allen et al., 1974a; Wolfe et al., 1974]. Kivelson [1976] analyzed the fluctuations observed in the buffer zone by P 10 and P 11 and described the region as a "layer of turbulence." The variance of the fluctuating field was found to decrease with increasing frequency, approximately as f^{-2}. V 1 and V 2 also observed high levels of field variability there, but it is not clear without further analysis that "turbulence" is the most accurately descriptive term for the observed fluctuations. Various models for the plasma motions in this outer region have been discussed by both Smith, Davis, and Jones [1976] and Kivelson [1976].

The Jovian magnetic tail

A major effort in the analysis and interpretation of the data obtained from the Pioneer spacecraft in the Jovian magnetosphere was directed towards a description of the characteristics of the magnetodisc current sheet. The magnetosphere was viewed as being dominated by this assumed axially symmetric distension of the near equatorial magnetic field containing enhanced plasma and energetic particle populations. On the P 10 outbound pass near the dawn terminator, the distortion of the magnetic field out of the magnetic meridian plane was viewed by some as a spiraling of the magnetic field due to a radial outflow of plasma or to waves in the magnetodisc itself [see Sec. 1.3 and Northrop, Goertz, and Thomsen, 1974; Kennel and Coroniti, 1975; Goertz, 1976b; Kivelson et al., 1978]. Smith et al. [1975] suggested, however, that the bending of field lines out of meridional planes was probably due to drag forces between the rapidly rotating magnetosphere and the slower magnetosheath flows.

The existence of a Jovian magnetotail of a few AU in length had been inferred by means of cosmic ray electron propagation studies [Krimigis et al., 1975; Mewaldt, Stone, and Vogt, 1976; Pesses and Goertz, 1976]. It was not until the V 1 observations at a local time of approximately 0400 that the existence and characteristics of the Jovian magnetotail were first identified by direct measurement [Ness et al., 1979a,b]. These results showed that the magnetic field at increasingly larger radial distances from the planet tended to lie parallel to the equatorial plane of Jupiter and also to the ecliptic plane, because the latter is inclined only 3° with respect to the former. More importantly, the azimuthal direction of the field showed an alignment paralleling the magnetopause surface, according to a reasonable model of the MP shape (see Sec. 1.4). These data were combined retrospectively with the P 10 results and compared to the geometry of the magnetic field in the dawn to midnight sector of Earth's magnetosphere. This comparison suggested that the transition of the field in the far magnetosphere near dawn to a magnetotail configuration was being observed. The V 2 results added substantially to a validation of this interpretation, showing that at a local time

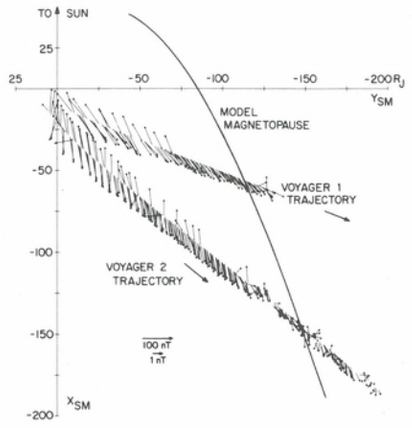

Fig. 1.28. Projection of hourly average magnetic field components on the solar magnetospheric (*SM*) *x–y* plane along the Voyager 1 and 2 outbound trajectories. Only the field vectors corresponding to alternate hours have been plotted for clarity. The data show that the field is distorted from magnetic meridian planes near the dawn terminator and bent back to parallel the magnetopause (MP) boundary. The MP shown is the Voyager 2 model boundary.

of ~0240 the magnetic field direction clearly indicated the sweeping back of magnetic fields lines into the tail region. Standard plots of 16 min average field magnitude, direction, and rms deviation for the complete tail passes of both V 1 and V 2 have been published by Behannon, Burlaga, and Ness [1981].

A clear visualization of the geometry of the field in the Jovian magnetotail region may be obtained by means of vector data plots. Figure 1.28 shows the projection on the *xy* plane of subsets of hourly averaged data obtained by the V 1 and V 2 spacecraft during their entire transits through the Jovian magnetosphere outbound from periapsis in March and July, 1979, respectively. The model MP shown corresponds to the surface determined by V 2 (see Sec. 1.4). A logarithmic scale has been used to represent field vector intensity. The coordinate system used is *solar magnetospheric*, in which the *x* axis points from the planet to the sun and the *z* axis lies in a plane defined by the *x* axis and the instantaneous position of the magnetic dipole axis. Close to the planet the field is seen to lie in magnetic meridian planes, although farther out the direction is best described as a sweeping back of of the field lines so as to parallel the magnetopause surface.

The companion views for these data are presented in Figure 1.29 and show the orientation of the magnetic field observed by V 2 in both the *xz* and *yz* projections. This figure also illustrates the differences between the tail and the magnetosheath (MS) fields. Following the initial entry of V 2 outbound into the MS, it found itself back inside the tail again for an extended period of time, out to a radial distance of $>250\ R_J$. There is essentially no difficulty in differentiating between MS and magnetotail fields on the basis of the high inclination of the sheath fields relative to the *xy* plane as illustrated by Lepping et al. [1981] (see last topic of this section).

The dominant variations observed by the Voyager spacecraft outbound at Jupiter to a distance of at least 140 R_J were produced by the recurrent passages through the tail current sheet, the motions of which are controlled by the ~10-hr planetary rotation period. Figures 1.28 and 1.29 illustrate these periodic traversals of the current sheet and the alternate location of the spacecraft in either the north or south tail lobe; this is identified more readily in Figure 1.28 by the changing polarity of the magnetic field. In Figure 1.29 the apparent excursion of the spacecraft in the *xz* and *yz* planes is due to the precessional motion of the magnetic dipole axis, which results from planetary rotation and tilt of the dipole axis to the rotation axis, and the subsequent rocking of the coordinate axes about the *x* axis. An alternative explanation for the observed magnetic field periodicities is that they are caused by a magnetic anomaly effect, which introduces asymmetries in the magnetic field and asserts an enhancement of plasma and energetic particle intensities over the longitudes of an active sector (region of anomalously weak magnetic field) in the northern hemisphere of Jupiter [Dessler and Vasyliunas, 1979; Vasyliunas and Dessler, 1981; and Chapts. 10 and 11].

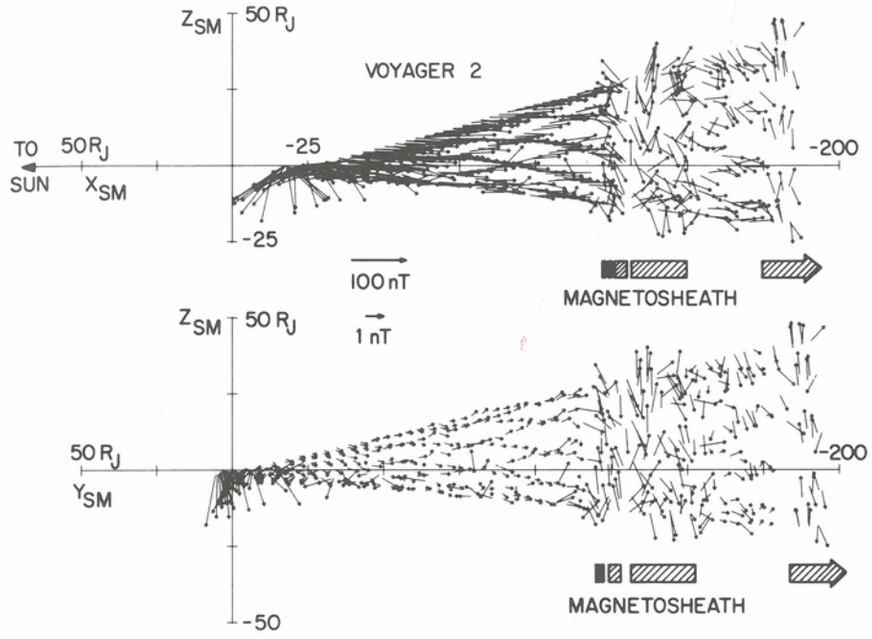

Fig. 1.29. Voyager 2 hourly average *SM x–z* (above) and *y–z* (below) magnetic field components. All hours have been plotted for more complete coverage in these views. Note in the upper panel the predominance of north lobe (outward-directed) fields as a result of the increasingly more northern location of the Voyager 2 outbound trajectory relative to the mean current sheet position. Also note in both panels the marked contrast between magnetosheath and tail field orientation, although during the more distant period in the tail more variation of the field was observed than in the near-planet region of the tail.

Field magnitude dependence on radial distance along the magnetotail

Detailed studies of the physical conditions leading to the development of a planetary magnetotail, its geometry and eventual disappearance or merging with the interplanetary medium require the knowledge of how the pressure balance is maintained or varies along the cavity-bounding surface, that is, the magnetopause. Of fundamental importance is the knowledge of the field magnitude dependence as a function of radial distance from the planet down the magnetotail. Analyses of this type have been performed for the Earth's magnetotail [Behannon, 1968; Mihalov et al., 1968] and yield a fall-off rate of the field intensity as a function of radial distance proportional to a power law, where the exponent was estimated to lie between -0.3 and -0.7. Similar studies have been conducted for the Jovian magnetotail using Pioneer and Voyager data.

The maxiumum hourly average field magnitude during each 10-hr period, B_{max}, was used to determine the radial variation of the total magnetic field as the V 1 and V 2 spacecraft traveled outbound from periapsis. A similar analysis was performed for

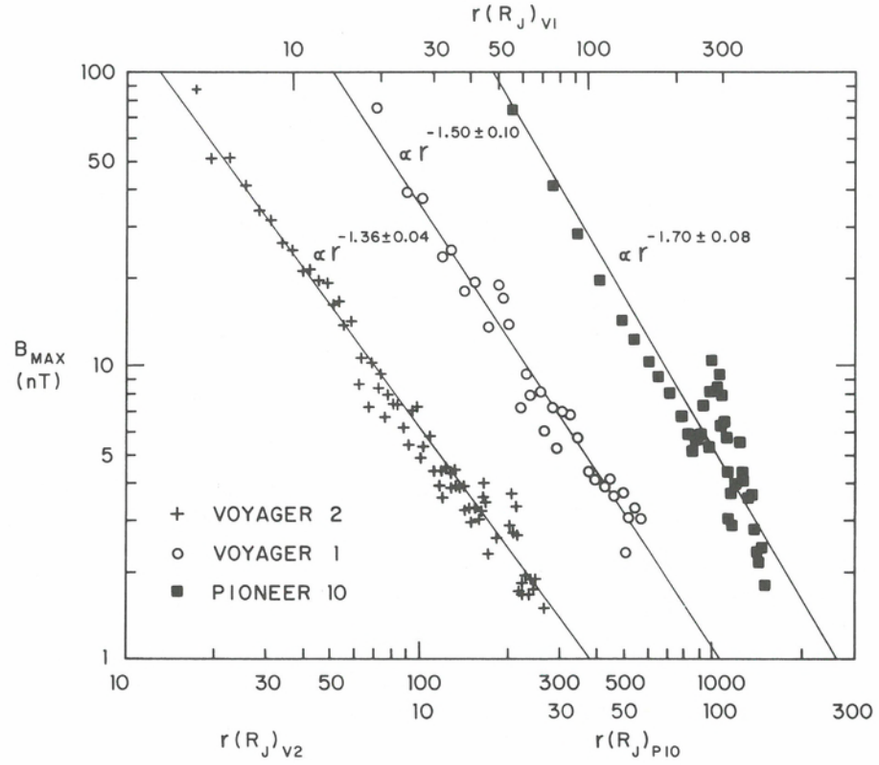

Fig. 1.30. Variation of average magnetotail lobe field with Jovicentric distance for Voyagers 1 and 2 and Pioneer 10. The observed variations are coded as indicated for the respective spacecraft. The least squares best fit inverse power law decreases are also shown in each case as solid curves. Best fit power law exponents are also given.

comparison purposes using P 10 data obtained from the NSSDC. The results are shown in Figure 1.30. A detailed description of the least-squares fitting procedure has been given in Behannon [1976], Appendix A.

For clarity of presentation, each of the three data sets have been separated along the abscissa and, as indicated, are to be referenced to radial distances scales that have been similarly shifted. The differing trends of the respective data sets reflect the different outbound trajectories, which had Sun–planet–spacecraft angles at the magnetopause of 99°, 115°, and 135° for P 10, V 1, and V 2, respectively. An indication of the degree of difference among individual gradients is given by the best-fit power law exponents, which were -1.70 for P 10, -1.50 for V 1, and -1.36 for V 2. There is no overlap in the standard error ranges on the three exponent values, suggesting that the difference between them is significant. These results indicate a departure from axial symmetry and require a tail-like current geometry. We note that the fall-off rates determined from these spacecraft observations are all steeper than those of the Earth's magnetotail.

There are systematic deviations from the simple power law dependencies. These effects are most noticeable in Figure 1.30 at and beyond $r = 100\ R_J$ in the V 2 and P 10 data. V 2 observed another, somewhat broader increase in the neighborhood of $r = 50\ R_J$ (see data in Behannon, Burlaga, and Ness [1981]), as did also the V 1 spacecraft. Although these features may well signify temporal variations, we cannot

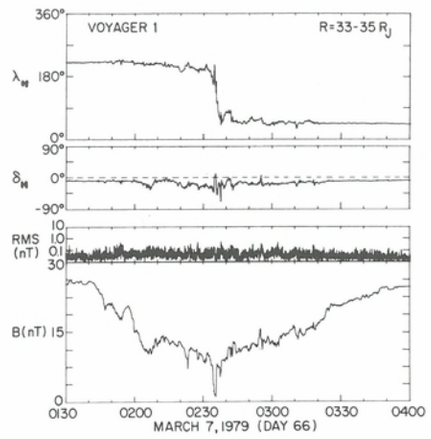

Fig. 1.31. Average magnitude, B, and direction, λ_H (longitude) and δ_H (latitude) of the magnetic field in heliographic coordinates (see text for definition) during a traversal of the current sheet by Voyager 2 at a radial distance of $\sim 34\ R_J$. Also given is the rms deviation of the total field over the 9.6 s averaging period.

uniquely separate temporal and spatial variations with single spacecraft traversals of the tail.

Tail current sheet observations

As in the case of the Earth, the Jovian magnetotail includes a large-scale current sheet separating the northern and southern lobes and across which the field reverses direction. Illustrating some of the general characteristics of this magnetotail current sheet, Figure 1.31 shows 2.5 hr of V 1 9.6 s average magnetic field data taken on March 7, 1979, during a crossing of the tail sheet at a Jovicentric distance of 34 R_J (and a distance of 22 R_J tailward of the dawn–dusk meridian plane). At the bottom is displayed the average field magnitude B, with the rms deviation of the field over the 9.6 s averaging period shown immediately above B. Note that the rms deviation is given on a logarithmic scale running from 0.01 to 10 nT. In the top half of the figure are shown the heliographic (HG) coordinate longitude and latitude angles λ_H, δ_H of the average vector field. By definition of the heliographic coordinate system, the angles λ_H, δ_H are given by

$$\lambda_H = \tan^{-1}(X_T/X_R)$$

and

$$\delta_H = \sin^{-1}(X_N/X)$$

where the spacecraft centered orthogonal unit vectors are defined with $\hat{R}$ along the Sun–spacecraft line, positive away from the Sun; $\hat{T}$ perpendicular to $\hat{R}$ and parallel to the Sun's equatorial plane, positive in the direction of planetary motion; $\hat{N} = \hat{R} \times \hat{T}$; and where

$$X = (X_R^2 + X_T^2 + X_N^2)^{1/2}$$

Figure 1.31 illustrates a classic traversal of a plasma sheet and embedded "neutral" sheet. In the field magnitude variation we see a broad and somewhat unsteady depression produced by the plasma sheet population of protons and ions of heavier nuclei as discussed by Lanzerotti et al. [1980]. At the minimum point of the depression is seen a relatively narrow (~ 2 min.), deeper depression simultaneous with the major variation in field azimuth, λ_H, and the largest negative deflections of the δ_H angle. Within this

narrower depression a minimum average field of ~1 nT was observed. The field was unsteady in direction as well as magnitude for most of the extent of the plasma sheet and tended to display an enhanced southward component throughout the plasma sheet region. The rms shows the increase in fluctuation energy within this region, although in this case the increase does not show up as dramatically as it would on a more expanded linear vertical scale.

Only approximately 25% of all Voyager sheet crossings resemble the example shown in Figure 1.31. Distant tail sheet crossings are more typically complex, consisting often of a series of partial or full traversals presumably caused by unsteady sheet motions. The fluctuations observed in the current sheet can at best be qualified as quasisinusoidal with amplitudes of ~1 nT and characteristic times ranging from 5 to 30 s.

Spectral analysis of the magnetic field in the *lobes* of the magnetotail, that is, the regions of the tail outside the plasma sheet, shows those regions to be magnetically quiet in general. Spectra computed over frequency ranges from 0.2 to 5 Hz had power spectral densities that are essentially at the Voyager magnetometer noise level ($\sim 1 \times 10^{-5} f^{-1}$ nT/Hz). These results are consistent with the extremely low plasma cutoff frequencies, corresponding to the electron concentrations of 10^{-5} cm^{-3} or less, found by the plasma wave experiment in the tail lobes [Gurnett, Kurth, and Scarf, 1980].

Voyager 2 magnetic field data obtained during crossings of the tail current sheet were analyzed by means of the minimum variance method of Sonnerup and Cahill [1967]. The objective was to determine the orientation, relative to the planet and the Sun, of the tail current sheet. The results, as discussed by Behannon, Burlaga, and Ness [1981], show that the normals are closely distributed in heliographic longitude about 90° and 270°, indicating that these normals oscillate primarily in the dawn–dusk meridian plane, with little tendency for pitching or oscillation in the forward (sunward) or tailward directions, and that they also tend to lie preferably in a fan centered on the normal to the heliographic equatorial plane ($\delta_N = 90°$). This result suggests that the tail current sheet tends to have a mean orientation approximately parallel to the heliographic equatorial plane (or the Jovigraphic equatorial plane, because the two planes were nearly equal at the time of the Voyager encounters). Motions of the sheet are limited primarily to oscillations about the planet–Sun line, with little evidence for rigid north–south motion or bending about the east–west axis.

Shape and motions of the Jovian current sheet

The literature contains several models of the current sheet treated as a mathematical surface and compared with P 10 observations. Four distinct approaches have taken the current sheet as (a) a rigid magnetodisc [Van Allen et al., 1974a; Goertz, 1976a], (b) a magnetodisc that bends over at distances beyond $r = r_0$ to become parallel to the planet's equatorial plane [Hill, Dessler, and Michel, 1974; Smith et al., 1975], (c) a rigid disc for $r < r_0$ with a propagating wave for $r \geq r_0$ [Northrop, Goertz, and Thomsen, 1974; Kivelson et al., 1978], (d) the same configuration as in (c) but with constant wave amplitude beyond $r = r_0$ [Eviatar and Ershkovich, 1976] and (e) a rigid disc but with longitudinally varying spiralling [Vasyliunas and Dessler, 1981]. Models (a) through (d) have been illustrated schematically by Carbary [1980]. All of these models except (e) have axial symmetry with respect to Jupiter's rotation axis, that is, they imply that all observers at a given distance from Jupiter would see the same sequence of current sheet crossings, except for a phase lag, regardless of their longitude. Observations of

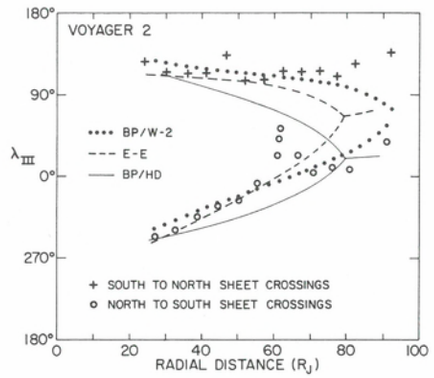

Fig. 1.32. System III longitude of Voyager 2 at the times of current sheet crossings as a function of radial distance from Jupiter, together with the predictions of three axial models (see text). The bent plane and the hinged-disc models predict a symmetry between the $S \rightarrow N$ and $N \rightarrow S$ crossings which is not observed.

current sheet crossings by V 1 [Ness et al., 1979a,b], which moved farther tailward than P 10, indicated that the axial models have limited applicability, and it was suggested that the current sheet on the night side is influenced by the formation of a tail as a result of the interaction of the solar wind with Jupiter's magnetosphere. V 2, which moved much farther tailward than V 1, provided further evidence against the early models and for the effects of a tail [Ness et al., 1979c; Bridge et al., 1979b]. Carbary [1980] reviewed the axial models referenced above and confirmed that they do not satisfactorily describe the times of the tail current sheet crossings observed by V 1 and V 2 (or, equivalently, the System III longitude at the time of a crossing as a function of the distance of the spacecraft from Jupiter); he showed that the model of Eviatar and Ershkovich [1976] gave a $\lambda_{III}(r)$ profile that qualitatively resembles the particle observations of current sheet crossings, but he did not show a fit of the model to the data.

Behannon, Burlaga, and Ness [1981] have used the measured times of the night side current sheet crossings determined by the magnetometers on V 1 and V 2 in an analysis that gives the best fit of those crossings to an assumed surface in order to evaluate and compare various models of the current sheet configuration, including both the published axial models (and some modifications of them) and some new (nonaxial) models which describe the effect of a tail configuration more explicitly. The axial model fitting results generally supported the conclusions of Carbary [1980]. Only the model of Eviatar and Ershkovich [1976] has been found to do a reasonably good job in modeling the observations, providing a fair fit to the V 1 crossings and a good fit to those of V 2. A modified model which allowed the wave to propagate from $r = 0$ rather than $r = r_0$ gave good fits to both data sets. The quality assessments were based on best-fit rms deviation values. Comparative results are illustrated in Figure 1.32 which shows the V 2 sheet crossing longitudes (System III) compared with curves predicted by the bent plane or hinged disc model (BP-HD), the limited-amplitude wave model of Eviatar–Ershkovich (E–E) and a model similar to the latter with wave propagating from the origin (BP/WP), which clearly gives a better fit (see also Chap. 5).

If the shape and position of the current sheet on the night side of the planet is influenced by the formation of a magnetotail, then there should be at least one nonaxial model which provides a still better global description of the current sheet surface, particularly at large distances in the tail. The simplest nonaxial model for a tail sheet is a plane surface that is approximately parallel to the Jovian equatorial plane and which rocks about the longitudinal axis of the tail as Jupiter's magnetic dipole axis cones about the rotation axis. More globally accurate would be a composite model that reduces to a rotating disc close to Jupiter and a rocking plane at large distances in the tail.

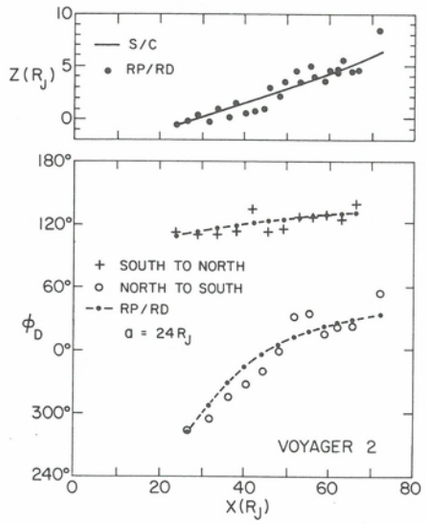

Fig. 1.33. Current sheet elevation (z) and azimuth of the dipole axis (ϕ_D) at the time of current sheet crossings are shown as functions of distance from Jupiter along $\hat{X}$, together with the predictions for these parameters based on a best fit to the rocking plane/rotating disc (RP/RD) model. This one-parameter model gives a good fit to the data over the range of distances that was considered.

The nonaxial data-fitting study considered both the simple rocking plane and the composite rocking plane/rotating disk (RP/RD), as well as variants of the latter with both longitudinal crosstail bending and wave propagation [Behannon, Burlaga, and Ness, 1981]. The coordinate system used in the analysis was a fixed Cartesian system with origin at Jupiter's center, $\hat{Z}$ northward along Jupiter's rotation axis, $\hat{X}$ radially away from the Sun, and $\hat{Y}$ completing the right-handed triad. Within a certain radial distance ($\sim 30\ R_J$), a rotating disc approximates the near-planet current sheet. The 1-parameter RP/RD model, which reduces to a rotating disc close to Jupiter and to the rocking plane at large distances, is a ruled surface given by

$$z/\tan\alpha = x\,\mathrm{sech}\,(x/a)\cos\phi_D + y\sin\phi_D$$

where α is the "hinge point" distance, and ϕ_D denotes the longitude of Jupiter's dipole axis relative to the tail axis at the time of the current sheet crossings.

Fits of the nonaxial models to the V 1 and V 2 current sheets crossings yielded results that ranged from fair for V 1 for both the rocking plane and the RP/RD models to good and very good, respectively, for the rocking plane and the RP/RD modeling of V 2 data. Fits with modified models also have shown that wave propagation is relatively unimportant for nonaxial models. Detailed descriptions of the models and tabulations of fitting results are given by Behannon, Burlaga, and Ness [1981].

The validity of the RP/RD model can be demonstrated by comparing the observed ϕ_D with the predictions of the RP/RD model. These results are shown in Figure 1.33 for the V 2 tail current sheet crossings. The model gives an excellent fit to both the south-to-north and the north-to-south crossings over the entire range of distances, $24\ R_J \lesssim x \lesssim 72\ R_J$. More distant crossings were not used in the analysis because of considerable temporal variation. Figure 1.33 also shows the observed z positions of the spacecraft at the times of the crossings as a function of x together with the predictions of the RP/RD model. The model gives a very good fit to $z(x)$, the scatter being only $\sim \pm 1\ R_J$. Although the results of applying statistical tests to the models suggest that the "best-fitting" axial and nonaxial models are equivalent in terms of "goodness-of-fit" [Behannon, Burlaga, and Ness, 1981], it should be noted that the simple nonaxial model has fewer parameters.

Because the data sets are rather restricted, it cannot be claimed that any one of the models is better than another. The foregoing exercise merely illustrates that a one-parameter nonaxial model fits the data, particularly that of V 2, with less deviation than a particular two-parameter axial model. The essential feature of these models seems to be that in the tail, the current sheet is extended parallel to the x axis with a limited elevation along z at distances $\gtrsim 30\ R_J$. It is interesting to note that none of the models tested gave as good a fit for V 1 as for V 2, suggesting that at the position of V 1 there were spatial distortions of the current sheet geometry that were not evident along the V 2 trajectory (see Behannon, Burlaga, and Ness [1981] for a comparison of the results of fitting the various models to the V 1 and V 2 data).

With the axial and nonaxial model it is assumed that the current sheet moves periodically, with a period $2\pi/\Omega$ equal to Jupiter's rotation period. For each model one can then predict the speed in the z direction as a function of position. The Voyager results suggest a maximum speed of the current sheet along z of $\lesssim 5\ R_J$/hr, depending on the maximum elevation of the sheet and on the spacecraft position. Using the RP/RD model, the thickness of the Jovian tail sheet was estimated by Behannon, Burlaga, and Ness [1981] under the assumptions that (a) the sheet motion was to a good approximation in the z direction, (b) the component of spacecraft velocity in the z direction was negligibly small, (3) the sheet motion during each traversal was steady. The latter is probably the weakest assumption. The average estimated thickness was $\langle\tau\rangle = 4.8 \pm 0.3\ R_J$ for 10 cases where the RP/RD model accurately predicted the z coordinate and ϕ_D. Using the average field strength observed during each of these crossings gives a sheet thickness range of 6–50 gyroradii (R_L) for 30 keV O^+ ions and greater by a factor of four for protons of the same energy. Such a sheet is relatively thin in comparison with the scale of the magnetotail, in contrast with the thickness of the terrestrial plasma sheet, which can be 40% of the radius of the tail. This result is consistent with the current sheet thickness estimate of $\sim 4.2\ R_J$ from plasma wave measurements [Barbosa et al., 1979] and with that the inner magnetosphere sheet model of [Connerney, Acuña, and Ness, 1981]; it is somewhat larger than the estimates of $\sim 1\ R_J$ by Smith et al. [1975] and 2.2–3.4 R_J by Kivelson et al. [1978] based on current sheet observations in other regions of the magnetosphere.

Bow shock and magnetopause shapes

The first detection of the Jovian bow shock and measurements of magnetosheath fields were performed by the P 10 and P 11 spacecraft [Smith et al., 1975; Davis and Smith, 1976]. The V 1 and V 2 encounters with Jupiter [Ness et al., 1979a,b] provided additional opportunities to investigate the physical characteristics of the planet's bow shock (BS), magnetosheath (MS), magnetopause (MP), and the outermost regions of the magnetosphere. The closest approach trajectories of V 1 and V 2 in Jupiter's orbital plane are shown in Figure 1.34. The times at which the two spacecraft crossed the BS and MP boundaries, as identified in the magnetic field measurements, were tabulated by Lepping, Burlaga, and Klein [1981]. Figure 1.35 shows magnetic field magnitude and root-mean-square (rms) deviation as functions of time for both V 1 and V 2 inbound at Jupiter from the preshock interplanetary magnetic field (IMF) through the BS and MP crossings to closest approach (CA). Both the number of crossings and the range of crossing positions observed in each case indicate significant variability in boundary locations. A marked variability in the BS and MP positions was also observed by the P 10 and P 11 spacecraft [Smith, Fillius, and Wolfe, 1978].

In the case of the Pioneers, published model BS and MP shapes were based on the gas dynamic analog and scaled from the Earth's boundaries to the actual Pioneer

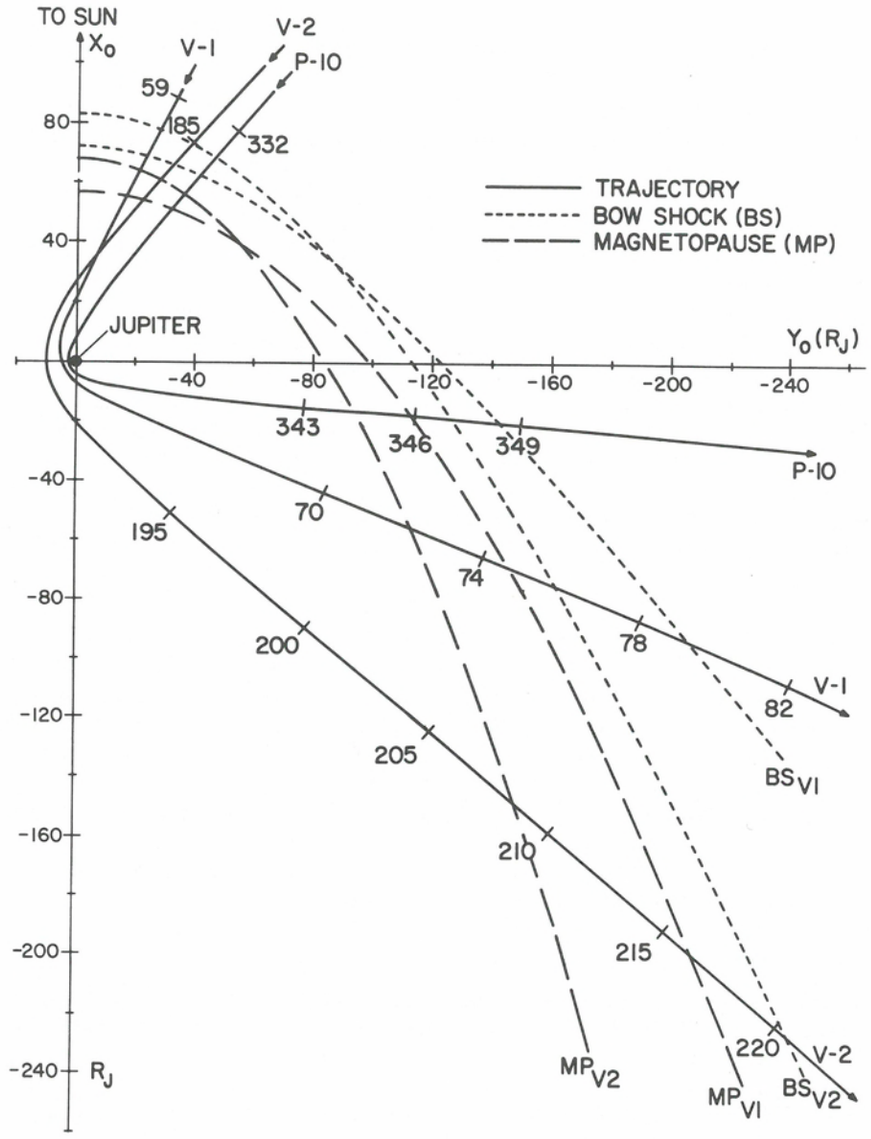

Fig. 1.34. The trajectories of Pioneer 10 and Voyagers 1 and 2 in the plane of Jupiter's orbit. Also shown are model magnetopause (MP) and bow shock (BS) boundaries (see text).

observations [Wolfe et al., 1974; Mihalov et al., 1975]. For each Voyager spacecraft encounter, model hyperbolic BS and parabolic MP curves were fitted to the average observed boundary positions [Lepping, Burlaga, and Klein, 1981]. These curves are also shown in Figure 1.34. The hyperbola and the parabola have been used successfully to describe mathematically the terrestrial BS and MP shapes, respectively [e.g., Fairfield, 1971]. Assuming that the BS is an axially symmetric hyperbola in the orbital

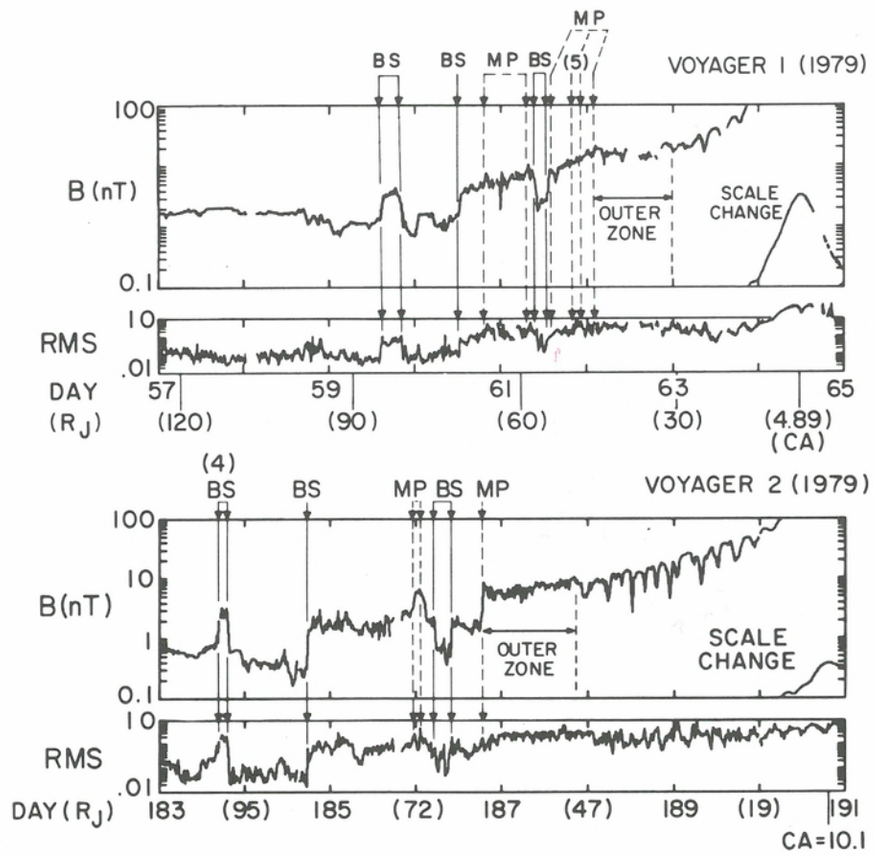

Fig. 1.35. Magnetic fields measured by Voyager 1 (above) and Voyager 2 (below) inbound at Jupiter to closest approach (CA). Given are the 16-min. average magnetic field magnitude B in nanoteslas (nT), field direction in heliographic longitude λ_H and latitude δ_H, and rms deviation in nT. λ is measured in a plane parallel to the sun's equator with $\lambda_H = 180°$ in the sunward direction. $\delta_H = 90°$ is northward with respect to that plane. Bow shock (BS) and magnetopause (MP) crossings are indicated (see text).

plane and that the MP is an axially symmetric parabola, and that these curves pass through the *average* Voyager boundary positions, the following curves resulted:

Voyager 1 MP: $y_0 = [168\,(57 - x_0)]^{1/2}$

Voyager 2 MP: $y_0 = [102\,(68 - x_0)]^{1/2}$

Voyager 1 BS: $y_0 = 0.712\,[(242 - x_0)^2 - 28{,}900]^{1/2}$

and

Voyager 2 BS: $y_0 = 0.380\,[(569 - x_0)^2 - 236{,}000]^{1/2}$

where x_0 and y_0 are coordinate positions relative to the planet-centered Jupiter Orbital Coordinate System in units of Jovian radii, and where $\hat{X}_0$ is positive sunward, $\hat{Z}_0$ is per-

Table 1.4. *Summary of Voyager boundary crossings*

	Bow shock				Magnetopause							
								Normal				
		Distance (R_J)			Distance (R_J)			Average	Est	Model		
Spacecraft	No	First	Last	No.	(No)*	First	Last	δ_H	λ_H	λ_H		
Voyager-1												
Inbound	5	86	56	9	(8)	67	47	3°	165°	168°		
Outbound	7	199	258	3	(3)	158	165	7°	124°	120°		
Voyager-2												
Inbound	7	99	66	3	(2)	72	62	−1°	155°	152°		
Outbound	9	282	>380	17	(2)	170	279	?	?	109°		

(No.)* refers to the number of well-estimated cases; see text.

pendicular to the planet's orbital plane, positive northward, and $\hat{Y}_0 = \hat{Z}_0 \times \hat{X}_0$. $\hat{X}_0$ defines the axis of symmetry. Because neither Voyager spacecraft traversed the duskside boundaries (which was also true for P 10 and P 11), little can be said about the duskside portions of the models. Aberration due to planetary motion with respect to the solar wind is negligible, but an asymmetry may still exist, at least at lower latitudes near Jupiter, because of the rapid rotation of the planet and plasma loading at lower latitudes.

Table 1.4 summarizes the number of BS and MP boundary crossings, both the total number in each case and for the MP crossings the number for which normals to the surface could be acceptably well estimated [Lepping and Behannon, 1980] using the Sonnerup and Cahill [1967] minimum variance technique; the latitude (δ_H) and longitude (λ_H) of the average of the "well-estimated" MP normals, and the longitude of the normal to the model MP are also given in HG coordinates. Table 1.4 shows that, except for the outbound V 2 MP crossings, the agreement between the average estimated and the model normals is quite good; it has been assumed that $\delta_H\{\text{Model}\} \equiv 0°$. Identification of the V 2 outbound MP traversals was based on rapid changes in field direction together with changes in 10–140 eV plasma electron flux and plasma ion density (J. Belcher and H. Bridge, private communication, 1980). Only two of the 15 crossings provided results consistent with the model normal. In almost all ($\gtrsim 87\%$) of the "well-estimated" MP cases, the boundary surface discontinuities were consistent with being tangential discontinuities according to the criteria of Lepping and Behannon [1980].

Magnetosheath field structure

The magnetic field in Jupiter's magnetosheath, particularly along the dawn magnetospheric flank, exhibits quasiperiodic variations in orientation that appear to be correlated with planetary rotation, and it is appropriate to include a brief description of the MS observations in this outer magnetosphere survey. Specifically, the fields observed by V 1 and V 2 outbound in the MS were oriented predominantly in a north or south direction and were found to vary between the two extremes of orientation with a quasiperiod of ≈ 10 hr, the Jovian rotation period [Lepping, Burlaga, and Klein, 1981; Lepping et al., 1981]. Examination of the P 10 MS outbound data has revealed a similar large-scale structuring of the MS in those observations, also. Similar directional changes in the field were observed by the Voyager spacecraft inbound through the MS near the MP, but the occurrence was much less frequent, no quasiperiodicity was apparent, and the scale lengths were on average much shorter. Highly inclined fields have also been observed occasionally in the Earth's MS, although to date there have been no reports of sheath field variations that are controlled by planetary rotation. Thus, the phenomenon detected at Jupiter may be unique to and characteristic of the Jovian system.

A broad view of the phenomenon is given in Figure 1.36, which shows the latitude (δ_H) of the magnetic field as observed by V 2 outbound for a period of approximately ten days. The data are plotted with respect to the System III (1965) longitude of the subspacecraft position, with two 360° cycles (plus 45° overlap) per panel. The calendar day (and fraction of a day) at the beginning of each panel is shown at the left. Periods during which the spacecraft reentered the magnetosphere or entered the solar wind are denoted by shading.

It can be seen in the figure that a significant number of field variation "events" occurred near $\lambda_{III} \approx 360°$ (indicated by vertical arrows at bottom). Although "events" occurred at other longitudes as well, there was no tendency for the events to cluster

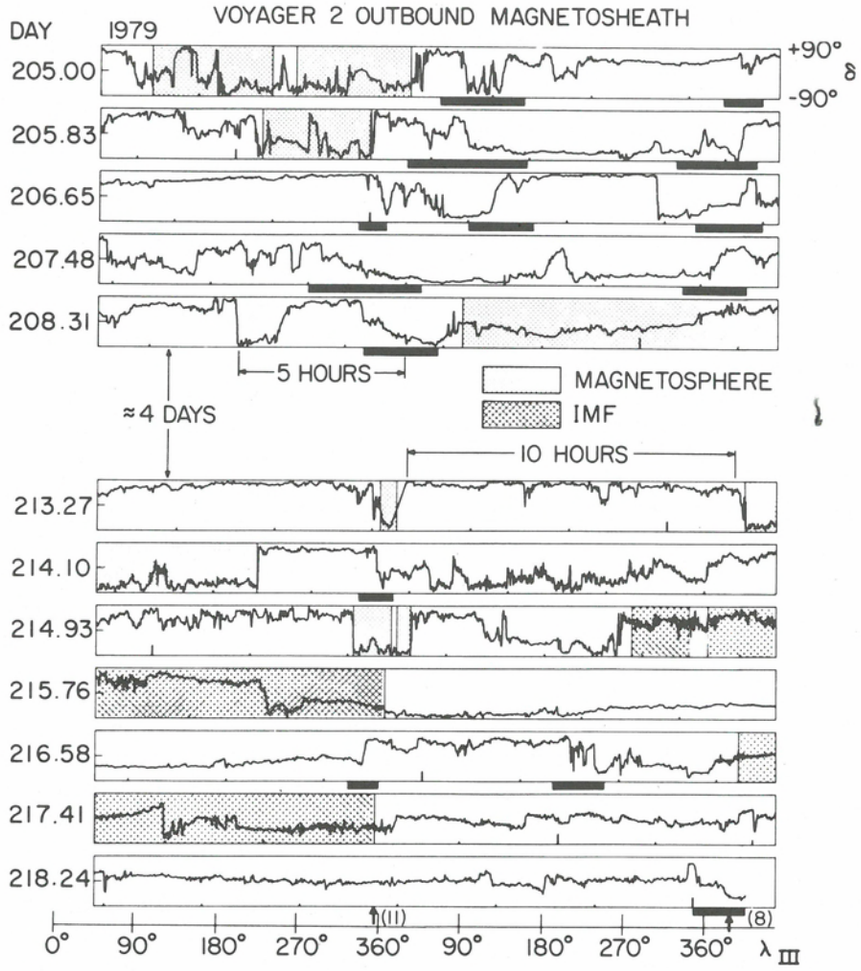

Fig. 1.36. Latitude (δ_H) of the magnetic field in the outbound MS along the Voyager 2 trajectory for a total of 12 Jupiter rotation periods; the central four days consisted primarily of magnetosphere data. Periods within the magnetosphere or in the interplanetary magnetic field (IMF) are denoted by shading. The data are plotted with respect to Jupiter's System III longitude of 1965.0 (λ_{III}) and day of the year, with major tick marks denoting starts of days.

about any longitude other than 360°. Here an "event" is defined as one of four occurrences: (1) a major north-to-south change of the latitude δ_H; (2) a major south-to-north change of δ_H; (3) a MP crossing; or (4) a BS crossing. Eleven such events occurred in association with the first arrow and eight with the second. This suggests a synchronization of field latitude changes and MP and BS motions jointly with the planetary rotation period of ≈ 10 hr (9.925 hours for System III, 1965). Some events also occur with a 5-hr period, but with a lower occurrence frequency. Note that there is much less variability in the later sheath measurements taken at greater distance from the MP.

A minimum variance analysis according to the method of Sonnerup and Cahill [1967] was carried out using 78 1-hr averages of V 2 sheath data and 64 V 1 1-hr averages [Lepping et al., 1981]. This analysis showed the tendency for the undulatory variations in the MS field to be contained in a plane which was nearly parallel to the local model MP for each data set analyzed. Similar analyses were carried out for portions of most of the large sheath field features individually using 48 s average V 1 and V 2 field data. The specific analysis intervals for V 2 are indicated by the black horizontal bars in Figure 1.35. With only a few exceptions, the individual minimum variance-estimated normals were found to cluster closely around the model MP normals.

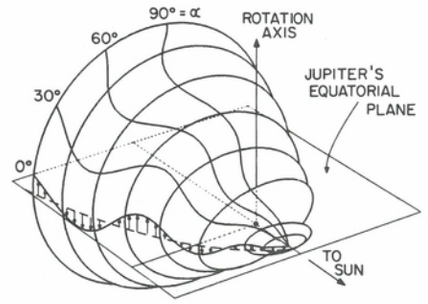

Fig. 1.37. A model of the dynamical magnetopause of Jupiter. The MP surface is shown here as it would be seen by an observer 30° away from the Jupiter–Sun line in the equatorial plane and 30° above that plane. It is assumed that near the vicinity of the nose of the magnetosphere the intersection of the MP surface with a plane perpendicular to the Jupiter-Sun line is an ellipse due to an internal disc-like current sheet. The ratio of the semimajor and semiminor axes was chosen equal to that given by Engle and Beard [1980] for the ellipse in the plane which contains the rotation axis. As the planet rotates, an ellipse near the nose oscillates about the Jupiter–Sun line. Information about the orientation of this ellipse propagates tailward at a speed which equals the sum of the Alfvén speed and the bulk speed in the magnetosheath near the MP (see text). The dashed line is the model MP derived from observed crossing positions [Lepping et al., 1980].

It was additionally found by Lepping et al. [1981] that the north–south component of the magnetic field observed outbound in the MS by V 1 and V 2 was strongly correlated with the north–south plasma velocity component. The components orthogonal to the north–south direction showed only weak correlations.

A plausible explanation for the observed phenomenon described briefly here can be formulated in terms of the draping of MS fields around a flattened (approximately in the $\hat{Z}_0$ direction) and dynamic Jovian magnetosphere, as suggested in the previous section. The motion and shape of such a magnetosphere depend on the rapid rotation of the current sheet within it. The flowing plasma in the MS is probably being deviated alternatively "northward" and "southward," as viewed in Jupiter's equatorial plane, primarily by the rocking motion of the magnetospheric current sheet about the Sun–Jupiter line. The field lines frozen into this deflected plasma are constrained to lie in a plane parallel to the MP, especially close to the MP, and to move with the plasma in a convected wave generated by the rocking motion of the magnetosphere (the geometry is illustrated in Fig. 1.37 and further described in the caption). Similarly, the quasi-periodic V 2 observation of the MP may be related to the motion and configuration of the magnetospheric current sheet, particularly that of the magnetotail current sheet. Pioneer observations suggested that the magnetospheric current sheet contributes a substantial disturbance field in Jupiter's outer magnetosphere [Smith et al., 1975]. The Voyager observations provide strong evidence that the effects of this current sheet probably extend beyond the magnetosphere into the magnetosheath.

Prior to the Voyager encounters with Jupiter, Dessler and Vasyliunas [1979] speculated that the preferential concentration of magnetospheric plasma within the active sector hypothesized in the magnetic anomaly model [Dessler and Hill, 1975] might have an observable influence on the location and motion of the MP. On this basis, a range, in λ_{III} (1965) coordinates, was predicted within which the Voyager MP crossings should occur. The longitude of greatest occurrence of V 2 outbound crossings, $\lambda_{III} \approx 360°$, lies just outside the range suggested by Dessler and Vasyliunas. A 2.5 hr delay ($\Delta\lambda_{III} \simeq 90°$) is required to force agreement. Following the Voyager encounters, Vasyliunas and Dessler [1981] have reiterated what had been stated as a qualifier in Dessler and Vasyliunas [1979]: that there is no clear theoretical basis for believing that the active sector can affect the MP, as for example, through the formation of an active sector-associated asymmetrical bulge in the MP surface. It is clear from the Voyager magnetometer results that a possible validation of the magnetic anomaly model of the Jovian magnetosphere will require further coordinated interdisciplinary studies and perhaps additional observations.

1.5. Summary

From the foregoing it is clear that significant progress has been made toward the understanding and modeling of the Jovian magnetosphere, both from an absolute knowledge point of view as well as from the standpoint of comparative studies of planetary magnetospheres in the solar system.

The largely complementary trajectories of the Pioneer and Voyager spacecraft have allowed the in situ exploration of a reasonably representative fraction of the Jovian magnetospheric cavity although the coverage of important regions is far from complete, as illustrated in Figure 1.34. The intrinsic planetary field outside $\sim 1.5\ R_J$ and the inner and middle magnetosphere, including the equatorial current sheet, are reasonably well understood on a global scale. The same applies to the large scale configuration of the magnetosphere, although this understanding is restricted to regions relatively close ($< 300\ R_J$) to the planet and our understanding is as yet qualitative. Much of the Voyager observations and the associated initial interpretations and models have yet to be fully digested. The retrospective and correlative studies that will necessarily be undertaken in the next few years will probably eclipse our present understanding quickly, as the pieces of the puzzle laid out in this volume are assembled. From the magnetic field point of view there remains, however, a large number of problems which require investigation; among these are: (1) the small scale geometry of the field near the surface and the large scale configuration of Alfvén standing waves in the Io torus which undoubtedly play a significant role in determining decametric emission characteristics; (2) additional studies concerning the electrodynamic interaction of satellites and rings with the corotating plasma; (3) large scale current systems in the magnetosphere and on its boundaries; (4) the adiabatic motion of charged particles in the Jovian magnetodisc; (5) self-consistent magnetic field/plasma models; (6) long term secular variations of the intrinsic planetary field; and (7) possible intrinsic magnetic fields of the Galilean satellites.

The polar regions remain largely unexplored except for remote optical and UV observations from spacecraft and ground-based observatories. These regions are certain to play a crucial role in the dynamics of the magnetosphere-solar wind interaction, as in the case of the Earth, and their study is of fundamental importance.

Future spacecraft placed in orbit around Jupiter will contribute essential data to carry out these studies. Ground-based observations will augment and complement spacecraft observations and will provide the long term observational baseline required

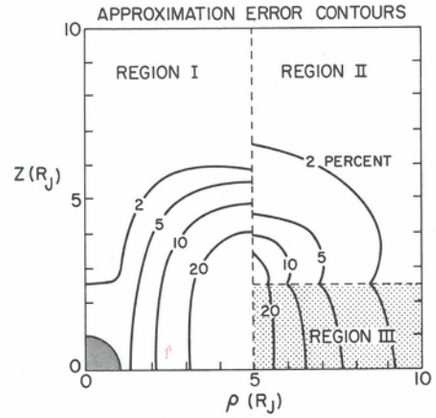

Fig. 1.38. Contour map showing maximum errors in current sheet model magnetic field components, B_ρ or B_z, in three regions of ρ, z space for which simple analytic forms exist.

to monitor large-scale changes in the morphology of the Jovian system as well as discover potentially new phenomena in the magnetosphere. These studies will contribute significantly to the understanding of our own Earth's magnetosphere and the general problem of the interaction of rapidly rotating magnetized bodies with stellar winds.

APPENDIX

For the purposes of computing the field due to the model current sheet the numerical integration of the integral results quoted by Connerney, Acuña, and Ness [1981] may be cumbersome. The following analytical approximations, applicable in the regions defined in Figure 1.38 can be used with negligible error except in the immediate vicinity of the inner sheet edge:

$0 \le \rho \le 30\ R_J;\ |z| \le 30\ R_J$

$$B_\rho^{I} = (\mu_0 I_0/2)\,(\rho/2)\,(1/F_1 - 1/F_2)$$

$$B_z^{I} = (\mu_0 I_0/2)\,\{\,5(z^2 + 5^2)^{-1/2} - (\rho^2/4)\,[\,((z-2.5)/F_1^3) - ((z+2.5)/F_2^3)\,]\,\} - B'_z$$

$$B_\rho^{II} = (\mu_0 I_0/2)\,\{\,(1/\rho)\,[F_1 - F_2 + 5] - (5^2\rho/4)\,[1/F_1^3 - 1/F_2^3]\,\}$$

$$B_z^{II} = (\mu_0 I_0/2)\,\{\,5[z^2 + \rho^2]^{-1/2} - (5^2/4)\,[\,(z - 2.5)/F_1^3 - (z + 2.5)/F_2^3]\,\} - B'_z$$

$$B_\rho^{III} = (\mu_0 I_0/2)\,\{\,(1/\rho)\,[F_1 - F_2 + 2z] - (5^2\rho/4)\,[1/F_1^3 - 1/F_2^3]\,\}$$

$$B_z^{III} = B_z^{II}$$

and

$$B'_z = (\mu_0 I_0/2)\,(1/10)$$

where in Region I:

$$F_1 = [(z - 2.5)^2 + 5^2]^{1/2}$$

$$F_2 = [(z + 2.5)^2 + 5^2]^{1/2}$$

and in Regions II and III:

$$F_1 = [(z - 2.5)^2 + \rho^2]^{1/2}$$

$$F_2 = [(z + 2.5)^2 + \rho^2]^{1/2}$$

With z and ρ in units of Jovian radii. A choice of $(\mu_0 I_0/2) = 225$ (150) corresponding to the V 1 (V 2) model of Connerney, Acuña, and Ness [1981] leads to a computed field in nanoteslas. The quantity contoured in Figure 1.38 is the percent error of the approximate solution for either B_ρ or B_z, whichever is greatest, determined by comparison of the computation using the approximate solutions given here and the appropriate numerical integration [Connerney, Acuña, and Ness, 1981].

ACKNOWLEDGMENTS

The authors are grateful to their colleagues N. F. Ness and A. W. Schardt, Editor A. J. Dessler, and two anonymous referees for their helpful comments and suggestions at various stages of the development of this review. We also thank wholeheartedly Barbara C. Holland for producing and correcting the typescript and Floyd H. Hunsaker and Larry A. White for producing most of the illustrations.

2
IONOSPHERE

Darrell F. Strobel and Sushil K. Atreya

Our understanding of Jupiter's ionosphere has been enhanced by the Voyager encounters. Vibrationally excited H_2 ($v \geq 4$) probably played an important role in providing a rapid loss mechanism for protons (the major topside ion) during the Voyager encounter. A straightforward calculation of the Voyager 1 entry electron concentration profile with chemistry and physics adequate to understand the Pioneer radio occultation profiles yields significant differences from the Voyager radio science measurements and suggests that substantial improvements in models may be necessary if the preliminary results of the observations remain unaltered after improved reduction and analysis of the data. It is argued that, although solar EUV radiation probably controlled the ionosphere during the Pioneer observations, particle precipitation as evidenced by strong H_2 airglow emissions on a planetwide basis appears to have played an essential role in both heating the thermosphere and as an ionization source during the Voyager encounters. The main contribution to the Pedersen conductivity in Jupiter's ionosphere occurs in the region where multilayer structure is dominant and accurate reductions of the Voyager radio occultation measurements are not yet available. Theoretical estimates of the integrated Pedersen conductivity are in the range of 0.02–10 mho; the former values are representative of an ionosphere produced by solar EUV radiation and the latter of the auroral ionosphere under intense particle precipitation.

2.1. Introduction

The original interest in an ionosphere on Jupiter was generated by the discovery of strong radio-frequency emissions at ~20 MHz that were thought to be plasma frequencies associated with Jupiter's ionosphere [Gardner and Shain, 1958]. A historical summary of developments in our understanding of Jupiter's ionosphere may be found in Strobel [1979]. The ionosphere of Jupiter provides a means to couple the magnetosphere to the atmosphere by virtue of its high conductivity and collisional interaction with the neutral atmosphere. The Pioneer and Voyager spacecraft have done much to stimulate interest in Jupiter's ionosphere by providing direct measurements of profiles of electron concentration at selected locations on Jupiter. Detailed measurements of ionospheric structure provide important information on the neutral atmosphere and physical processes that affect its structure in addition to data of purely ionospheric interest. Because a number of reviews on Jupiter's ionosphere have appeared previously [Hunten, 1969; McElroy, 1973; Huntress, 1974; Atreya and Donahue, 1976; Strobel, 1979], this chapter emphasizes the contributions from the Voyager program to our understanding of Jupiter's ionosphere.

2.2. Basic principles

The most fundamental quantities needed to understand the ionosphere are the electron and ion concentrations as a function of altitude, latitude, and, in the case of Jupiter, longitude. They are solutions of the electron continuity equation

$$\frac{\partial n_e}{\partial t} + \nabla \cdot \bar{\phi}_e = P_e - \alpha n_e^2 \tag{2.1}$$